ResearchGate

See discussions, stats, and author profiles for this publication at: https://www.researchgate.net/publication/330224665

Modeling of the disk nozzle parameters in biodiesel production

Article *in* International Journal of Renewable Energy Research · December 2018

CITATION
1

READS
123

5 authors, including:

Gennadii Golub
National University of Life and Environmental Sciences of Ukraine
58 PUBLICATIONS **187** CITATIONS
SEE PROFILE

Savelii Kukharets
Vytautas Magnus University
64 PUBLICATIONS **231** CITATIONS
SEE PROFILE

Oleksandr Medvedskyi
Polissia National University, Ukraine, Zhytomyr
17 PUBLICATIONS **27** CITATIONS
SEE PROFILE

All content following this page was uploaded by Savelii Kukharets on 12 January 2019.

The user has requested enhancement of the downloaded file.

Modeling of the Disk Nozzle Parameters in Biodiesel Production

Gennadii Golub*, Savelii Kukharets**‡, Yaroslav Yarosh***, Vyacheslav Chuba* and Oleksandr Medvedskyi***

*Department of Tractors, Automobiles and Bioenergy Systems, National University of Life and Environmental Sciences of Ukraine, Heroev Oborony Str., 15B, Kyiv, 03040, Ukraine

**Department of Mechanical and Engineering Agroecosystems, Zhytomyr National Agroecological University, Staryi blvd., 7, Zhytomyr, 10008, Ukraine

***Department of Processes Machinery and Equipment in Agrarian Engineering, Zhytomyr National Agroecological University, Staryi blvd., 7, Zhytomyr, 10008, Ukraine

(gagolub@ukr.net, saveliy_76@ukr.net, yaroslav.yarosh76@gmail.com, vvchuba@ukr.net, aleksmedvedsky@gmail.com)

‡Corresponding Author; Savelii Kukharets, Zhytomyr National Agroecological University, Staryi blvd., 7, Zhytomyr, 10008, Ukraine, Tel: +38 067 665 3548, saveliy_76@ukr.net

Received: 20.08.2018 Accepted:04.11.2018

Abstract - The design and the technological parameters of the disk nozzle and circulation reactor for biodiesel production are established. The basis of the research is to determine the effective length of the emulsion flow in turbulent regime with minimal energy consumption. The effective length of the emulsion flow was determined on the basis of determination of the axial velocity in the flow sections at different distances from the nozzle. The value of the average axial velocity was carried out using the principle of conservation of the kinetic energy of the flow with the determination of the kinetic energy of the annular elements of the emulsion flow at the beginning and at the end of the flow. To conduct the experimental studies of changes in the emulsion flow rate, a specially designed plant was used, which consisted of a disk nozzle, a working capacity and a hydroelectric station. The conducted research allowed to coordinate the design and the technological parameters of the circulation reactor for high-quality biodiesel production with minimal energy consumption.

Keywords - Transesterification, emulsion, turbulent regime, power consumption, clearance, depth of immersion.

1. Introduction

Significant emission of greenhouse gases from the burning of fossil fuels (natural gas, diesel fuel, coal, etc.) encourages people to switch to renewable energy sources [1, 2]. A range of new equipment types has emerged, which use biodiesel [3].The production and the use of biodiesel can increase the level of energy autonomy of agricultural production [4]. Biodiesel can be produced from different sources such as vegetable oils, animal fat [5] and waste cooking oil [6]. Using biodiesel in the production of agricultural products reduces emissions of carbon dioxide (CO_2) [7], nitrogen oxides [8] sulfur compounds, soot, and hydrocarbons [9].

Biodiesel is mainly produced in the process of transesterification [10] of vegetable oil with methyl alcohol [11] with a catalyst [12]. Methyl alcohol, oil and catalyst form a multiphase emulsion in which the reaction is slowed down due to the small area of the interphase contact of the components [13]. To accelerate the transesterification reaction, the necessary formation of an emulsion with an increased contact area of the components is required, which is achieved by constant mixing [14]. Due to the mixing, the quality of transesterification process can be achieved. [15]. The quality of the transesterification reaction depends on hydrodynamic conditions and requires mixing with the corresponding intensity [16, 17].

The most widely used reactors for the transesterification process are equipped with mechanical mixers [18]. The mathematical model of the transesterification process for biodiesel production based on the fuzzy logic theory has been designed. [19]. The simulation of the technological process of transesterification of vegetable oils in batch reactors [20] was carried out. However, in biodiesel

production there are problems associated with the mixing of emulsion components in the process of transesterification, such as a significant duration of the process, the destruction of the required contact surface area of reagents, and a significant energy consumption.

For biodiesel production, the fermentation reactors of conventional [21] and rotating [22] types are often used, but they are of low productivity. Due to the insufficient efficiency of mixing, the transesterification process is not fully implemented and therefore additional washing [23] and purification [24] operations are used, which complicate the technological process of obtaining biodiesel in agricultural production.

In studies on the use of film [25] and tubular mixers [26] based on cavitation [27] or ultrasound [28], it is shown that the rate of the process of transesterification increases if small amounts of reacting substances (emulsion components) are mixed. However, such technologies of biodiesel production are characterized by high specific energy consumption.

Similar results regarding the efficiency of a mixing process are achieved in reactors with nozzles [29] and the circulation of the emulsion in a closed circuit [30]. With hydraulic mixing, the efficiency of the transesterification process is maintained when the turbulent regime is present in the emulsion jet [31]. The use of plants with hydraulic emulsion mixing and circulation allows the processes of transesterification and settling to be carried out in one vessel (container). However, during the operation of such a reactor, it is possible to form areas of emulsion stagnation. Besides, the issue of safe removal of biodiesel obtained during the reaction has not been resolved.

The analysis allows us to conclude that the existing and promising equipment for the biodiesel production does not fully ensure the efficiency of the technological process in agricultural production. There is a need for theoretical substantiation and experimental study of the parameters of the equipment for the biodiesel production when using hydraulic mixing.

2. Materials and Methods

A circulation reactor is proposed for the process of transesterification of vegetable oils (Fig. 1), which provides the repeated pumping of the emulsion in a closed loop. The disk nozzle is installed in the upper part of the reactor with the possibility of its movement along the reactor axis.

When the emulsion passes through the disk nozzle, a turbulent flow is created, which provides the necessary efficiency of the emulsion mixing in a fixed-height layer. By pumping the emulsion from the bottom of the mixer, the layer of the mixed emulsion is lowered, the mixing intensity is reduced and then the process of transesterification takes place.

The flow of the emulsion flowing out of the disk nozzle expands along the perimeter, forming a circular, prismatic in section, discharge pattern. This is because the emulsion flow portion flows out of the nozzle, pushing the portion of the emulsion that is in the vessel before the nozzle. And the emulsion layers around the flow, due to the viscosity action, are involved in the flow movement. Based on the condition of continuity of the flow [32, 33], the emulsion flow rate in all sections of the nozzle was the same and equaled the productivity (supply) of the hydraulic pump Q_0.

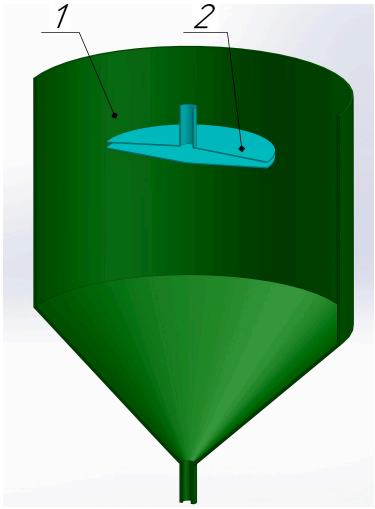

a)

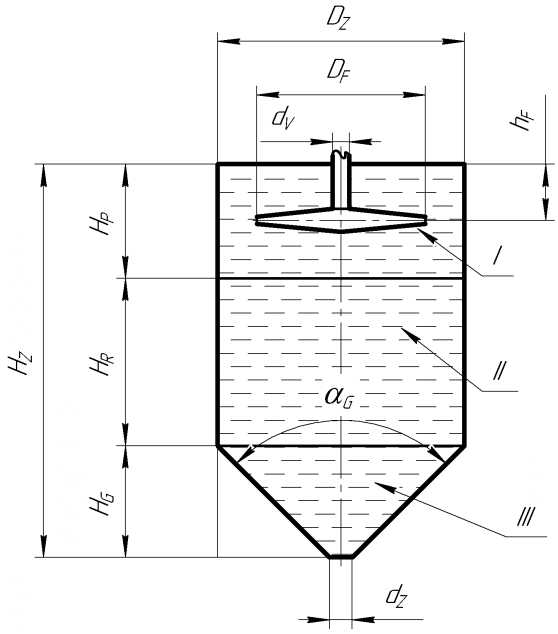

Fig. 1. The circulation reactor: a) – 3-D model, b) – block scheme; 1 – disk nozzle; 2 – reactor; I – the mixing area; II – the reaction area; III – the area of glycerin upholding; H_z– the reactor height, m; H_p – the height of the mixing area, m; H_r – the height of the reaction area, m; H_g – the height of the glycerin settling, m; D_z – the working diameter of the reactor, m; D_f – the nozzle diameter, m; h_f – the height of the nozzle installation, m; d_V – the diameter of the nozzle inlet, m; d_z – the diameter of the emulsion pumping hole, m

Two ring prismatic in the cross section of the emulsion flow elements were theoretically analyzed (Fig. 2, a) with the width l_0, at the beginning of the flow (at the outlet of the nozzle) and at the end of the flow at a distance l_x from the injector nozzle (Fig. 2, b).

In order to avoid additional loss of pressure in the middle of the nozzle, it was made in the form of cones without a bottom, which are combined with each other by their bases in such a way that they form a slit for the output of the circular flow of the emulsion. It allows to keep a constant emulsion speed υ0 in all internal circular cross sections of the nozzle.

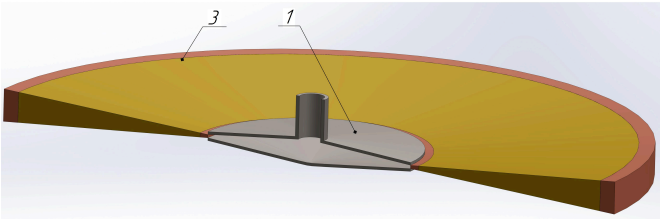

a)

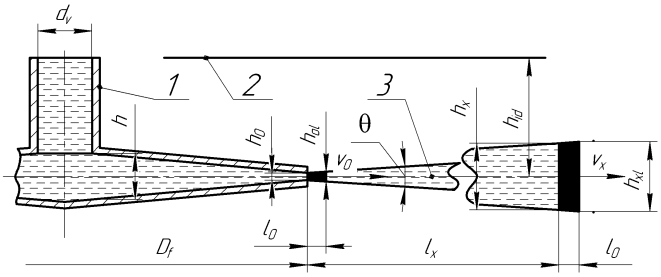

b)

Fig. 2. Disk nozzle: a) model, b) scheme; 1 – disk nozzle; 2 – the free emulsion surface; 3 – emulsion flow; h_0 – the final gap between the nozzle disks, m; h_x – the initial height of the final flow section, m; h_{0l} – the final height of the initial flow section, m; h_{xl} – the final height of the final flow section, m; l_x – the length of the emulsion flow, m; l_0 – the width of the studied annular in the emulsion flow, m; D_f – the nozzle diameter, m; d_V – the diameter of the nozzle inlet, m; θ – the flow expansion angle, rad; υ_0 – the emulsion axial velocity at the beginning of the flow, m/s; υ_x – the emulsion axial velocity at the end of the flow, m/s; h_{id} – the nozzle immersion depth, m

An experimental plant was developed to study the energy efficiency of circulating reactors equipped with a disk nozzle and the dynamics of the emulsion flow (Fig. 3, a). It contained: a disk nozzle (Fig. 3, b) with the diameter of 0.32 m, working capacity, hydraulic station for emulsion transfer, frequency converter Hitachi-3G3JX-A4075-EF, digital analyzer of energy consumption parameters DMK-30, tachometer UT-372. The hydroelectric station contained: gear pump NSh-100, asynchronous electric motor AIP-112-M4 with a capacity of 5.5 kW and a rated speed of 1500 rpm, a system of hoses and pipes. The frequency of rotation of the hydro station electric motor was regulated by the frequency converter Hitachi-3G3JX-A4075-EF and measured by the tachometer UT-372, the power consumption of the hydro station was determined according to the DMK 30 analyzer readings.

For experimental studies, sunflower oil was used, which pre-filled the working capacity at a certain height.

During the experiments the clearance between the nozzle disks h_0, the depth of immersion of the nozzle hid, the speed of the hydraulic pump rotation n and the power consumption N of the electric motor during the operation of the disk nozzle, and the speed of the emulsion jet in the range of distances from the beginning of the flow l_x=0...0.3 m were changed.

a)

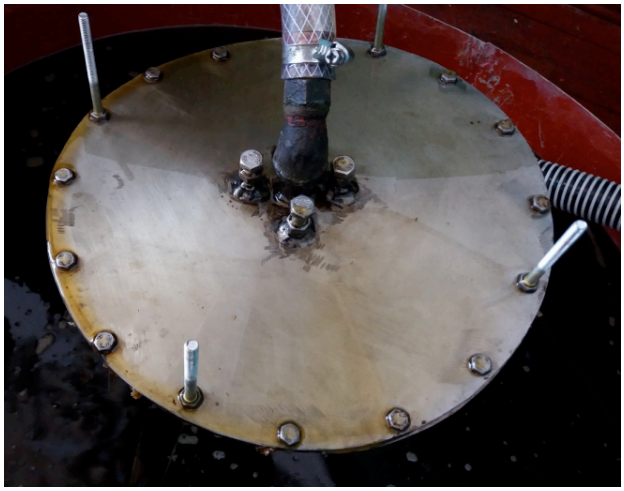

b)

Fig. 3. The plant for experimental studies of the disk nozzle (a) and the disk nozzle (b)

The velocity of the jet was determined by the formula:

$$\upsilon = \sqrt{2gH_\upsilon}, \quad (1)$$

Where H_υ – the velocity head in the emulsion flow, m.

The velocity head H_υ was defined with the help of piezometric pipes (Fig. 4) and was equal to the emulsion height in the tube above the free surface.

The intervals of the studied values are given in Table 1. For research D-optimal Box-Behnken plan was used.

Table 1. Intervals of values and levels of variation of the studied parameters

Parameter name and designation	Factor levels			Variation intervals
	-1	0	+1	
The speed of the pump rotation *n, min*$^{-1}$	300	850	1400	550
Nozzle immersion depth h_{id}, *mm*	7	27	47	20
The clearance between the nozzle disks h_0, *mm*	2	4	6	2

a)

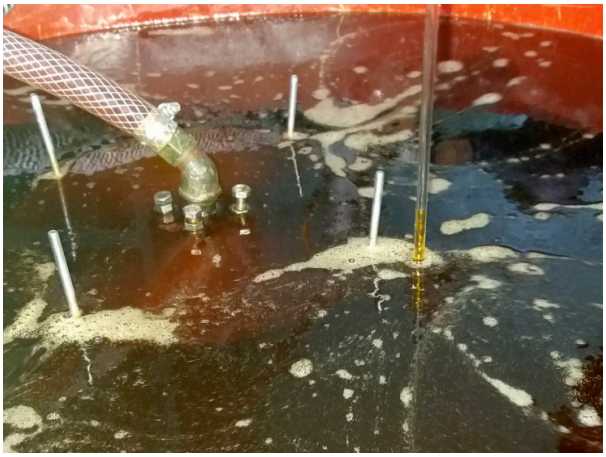

b)

Fig. 4. Piezometric pipes (a) and measuring the emulsion flow rate (b)

The obtained data were processed using specially developed software for the analysis of multifactor experiments. The homogeneity of the dispersion of the experimental data was evaluated by the Cochran criterion, the significance of the regression equation coefficients was evaluated by the Student criterion, and the adequacy of the obtained regression equation was evaluated by Fisher's ratio test.

3. Results and Discussions

3.1. Theoretical studies of the disk nozzle

We write the flow equation as the difference of kinetic energies in the annular elements at the beginning and at the end of the flow:

$$\frac{m_0 \upsilon_0^2}{2} - \frac{m_x \upsilon_x^2}{2} = \sum A_o - \sum A_x , \qquad (2)$$

where: υ_0 – the emulsion axial velocity at the beginning of the flow, m/s; υ_x – the emulsion axial velocity at the end of the flow, m/s; m_0 – the mass of the emulsion annular at the beginning of the flow, kg; m_x– the mass of the emulsion annular at the end of the flow, kg; ΣA_0 – the sum of forces at the beginning of the emulsion flow, J; ΣA_x – the sum of forces at the end of the emulsion flow, J.

We assume that the flow of the emulsion is counteracted by the hydrostatic pressure force F_p, the hydraulic friction force F_t, and the force of the hydraulic resistance F_t (Fig. 5). With this in mind, the equation (2) is rewritten as follows:

$$\frac{m_0 \upsilon_0^2}{2} - \frac{m_x \upsilon_x^2}{2} = l_0 \left(F_{p0} + F_{o0} + F_{t0}\right) - \\ -\left(l_x + l_0\right)\left(F_{px} + F_{ox} + F_{tx}\right) \qquad (3)$$

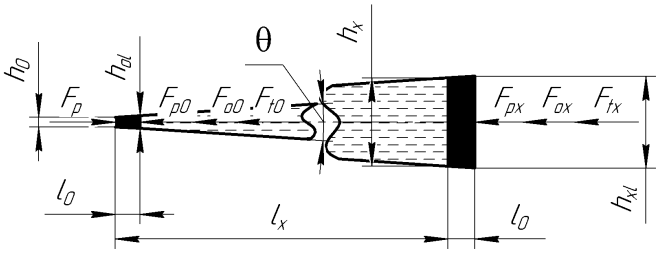

Fig. 5. The scheme of the main forces acting in the emulsion flow elements: F_{p0} – the power of hydrostatic pressure at the beginning of the flow, H; F_{px} – the power of hydrostatic pressure at the end of the flow, H; F_{t0} – the hydraulic friction force at the beginning of the flow, H; F_{tx} – the hydraulic friction force at the end of the flow, H; F_{o0} – the hydraulic resistance force at the beginning of the flow, H; F_{ox}– the hydraulic resistance force at the end of the flow, H; F_P – the force of the pump hydraulic pressure, H

The calculation formulas for the forces that counteract the movement of the emulsion flow are presented in table 2.

Table 2. Forces that counteract the movement of the emulsion flow

The force name	At the beginning of the flow	At the end of the flow
Hydrostatic pressure force, H	$F_{p0} = A_{l0}\rho g h_{id}$	$F_{px} = A_{lx}\rho g h_{id}$
Hydraulic friction force, H	$F_{t0} = k_t \eta A_{s0}$	$F_{tx} = k_t \eta A_{sx}$
Hydraulic resistance force, H	$F_{o0} = \frac{k_o \rho \upsilon_0^2 A_{l0}}{2}$	$F_{ox} = \frac{k_o \rho \upsilon_x^2 A_{lx}}{2}$

Where: ρ – the emulsion density, kg/m^3; g – the gravity acceleration, m/s^2; h_{id} – the nozzle immersion depth, m; k_0 – the hydraulic resistance coefficient, m/m; k_t – the viscous friction coefficient, s^{-1}; η – the emulsion dynamic visc, Pa·s; υ_0 – the emulsion axial velocity at the beginning of the flow, m/s; υ_x – the emulsion axial velocity at the end of the flow, m/s;

The calculation formulas for the areas that are included in the formulas in table 2 are shown in table 3.

Table 3. Calculation formulas of the areas of the emulsion flow

Name	At the beginning of the flow	At the end of the flow
Head resistance area, m^2	$A_{lo}=\pi\times\left(h_0+2l_0\tan\frac{\theta}{2}\right)\times\left(D_f+2l_0\right)$	$A_{lx}=\pi\times\left(h_0+2\left(l_x+l_0\right)\tan\frac{\theta}{2}\right)\times\left(D_f+2\left(l_x+l_0\right)\right)$
Friction area (lateral surface area), m^2	$A_{s0}=\frac{2\pi l_0\left(D_f+l_0\right)}{\cos\left(0{,}5\theta\right)}$	$A_{s0}=\frac{2\pi l_0\left(D_f+2l_f+l_0\right)}{\cos\left(0{,}5\theta\right)}$

The masses of the annular elements at the beginning and at the end of the flow were found by the formulas:

$$m_o=\pi\rho l_0\left(D_f+l_0\right)\left(h_0+l_0\tan\frac{\theta}{2}\right), \quad (4)$$

$$m_x=\pi\rho l_0\left(D_f+2l_x+l_0\right)\left(h_0+\left(2l_x+l_0\right)\tan\frac{\theta}{2}\right). \quad (5)$$

The axial velocity of the emulsion at the beginning and at the end of the flow was found by the formulas:

$$\upsilon_0=\frac{Q_0\eta_f}{\pi D_f h_o}, \quad (6)$$

$$\upsilon_x=\sqrt{\frac{m_0\upsilon_0^2-2\left(\begin{array}{l}l_0\left(F_{p0}+F_{o0}+F_{t0}\right)-\\-\left(l_x+l_0\right)\left(F_{px}+F_{ox}+F_{tx}\right)\end{array}\right)}{m_x}}. \quad (7)$$

The solution of the equation (7) taking into account the parameters given in the tables 1 and 2 and equations (4-5) allow us to determine the change in the axial flow rate of the emulsion according to its length depending on the supply of the hydraulic pump Q_0, the dynamic viscosity η, the emulsion density ρ, the depth of immersion of the disk nozzle hid, and the clearance between the nozzle disks h_0.

Taking the hydraulic radius of the emulsion flow as for the rectangular cross section [29, 30], it is possible to specify the emulsion flow effective length l_{xe} where mixing will occur with the required intensity, that is, when the Reynolds number Re≥2,320 is determined by a well-known equation:

$$\mathrm{Re}=\frac{4\upsilon_x R_g\rho}{\eta}, \quad (8)$$

Where the hydraulic radius was found by the formula:

$$R_g=\frac{\pi\left(D_f+2\left(l_x+l_0\right)\right)\left(h_0+2\left(l_x+l_0\right)\tan\frac{\theta}{2}\right)}{2\left(D_f+h_0+2\left(l_x+l_0\right)\left(1+\tan\frac{\theta}{2}\right)\right)}. \quad (9)$$

Considering that the pump speed linearly affects its supply (performance):

$$Q_0=q_o n_g, \quad (10)$$

where: q_o – the working volume of the hydraulic pump, м^3; n_g – the speed of the pump, c^{-1}.

The solution of the equation (3) with the parameters given in the tables 2 and 3 and equations (4-6) allows us to set the speed of the pump to provide the required emulsion flow length depending on the depth of the nozzle immersion and the clearance between the nozzle disks.

The solution of the equation (3) allows to determine the effective emulsion flow length ($l_e=l_x+2l_0$), find the necessary value of the pump supply and agree the design and technological parameters of the circulating reactor for biodiesel production.

3.2. Experimental study of disk nozzle

The results of experimental studies are presented in table. 4. The Cochran criterion equaled to G=0.082 and was less than its table value G_T=0.335 with 95% confidence. This indicates the homogeneity of the experimental data dispersion. The Fisher criterion at 95% confidence probability equaled to F=2.37 and was less than its table value F_T=2.53, which indicates the adequacy of the obtained regression equation.

As a result of the analysis of experimental studies of the relationship between the pump speed n (min^{-1}), the depth of nozzle immersion h_{id} (mm) and the clearance between the nozzle disks h_0 (mm) and the power consumed by the electric motor of the hydroelectric station N (W) and the speed υ_0 (m/s) of the emulsion jet at the nozzle exit, the corresponding empirical dependences were obtained:

$$N=625.5739-1.0322n+0.0017n^2, \quad (11)$$

$$\upsilon_0=2.4301+0.001n-0.9657h_0+0.0904h_0^2 \quad (12)$$

It was found that the power consumption is significantly affected by the speed of the pump, and the initial flow rate of the emulsion is affected by the speed of the pump and the clearance between the nozzle disks.

The dynamics of power change depending on the speed of the pump motor is shown in Fig. 6. The graph shows that the minimum power of 466 W is observed at a minimum pump speed of 300 min^{-1}, with an increase in the pump speed up to 1400 min^{-1}, the power increases in parabolic dependence and reaches the maximum value of 2460 W.

Table 4. Values of the set and measured values during the study of the disk nozzle

№	Pump speed, min^{-1}	Immersion depth, mm	Nozzle clearance, mm	Power, W	Flow rate, m/s		
					Flow length, cm		
					0	15	30
	n	h_{id}	h_0	N	v_0	v_{15}	v_{30}
1	1400	47	4	2475	1.469	0.28	0.198
2	300	7	4	470	0.280	0.198	0
3	1400	7	4	2500	1.534	0.313	0.14
4	300	47	4	475	0.343	0.198	0
5	1400	27	6	2470	1.329	0.343	0.14
6	300	27	2	470	1.172	0.28	0.198
7	1400	27	2	2400	2.078	1.01	0.485
8	300	27	6	465	0.243	0.14	0
9	850	47	6	955	0.886	0.14	0
10	850	7	2	1010	1.981	0.980	0.42
11	850	47	2	955	1.657	0.28	0.198
12	850	7	6	960	0.578	0.198	0
13	850	27	4	960	0.767	0.198	0.14
14	850	27	4	955	0.886	0.28	0.198
15	850	27	4	965	0.886	0.28	0.198

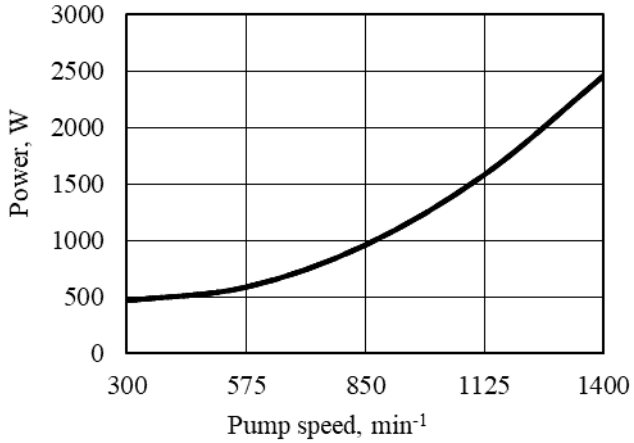

Fig. 6. Dependence of the power consumption by a hydroelectric power plant while a disk nozzle is operating, on the pump engine rotations

On the basis of equation (12) the graphical dependence of the emulsion flow velocity at the exit of the nozzle depending on the speed of the pump of the hydro station and the clearance between the nozzle disks has been obtained. Analysis of the equation (12) and the graph in Fig. 7 allows us to make conclusion as for the linear nature of the dependence of the flow rate at the exit of the nozzle on the pump speed. The minimum flow rate at the exit of the nozzle was 0.24 m/s and was observed at the clearance between the nozzle disks of 6 mm and the speed of the hydro station pump of 300 min^{-1}. The maximum flow rate was 2.08 m/s at a clearance of 2 mm and the speed of the hydro station pump of1400 min^{-1} (Fig. 8).

Regarding the effect of the clearance between the nozzle disks on the initial emulsion flow rate, it was found out that the decrease in the flow rate with an increase in the clearance between the nozzle disks occurs by parabolic dependence. When a clearance is bigger than 5 mm, the initial velocity of the emulsion flow becomes stable and remains practically unchanged with further increase of the clearance between the nozzle disks.

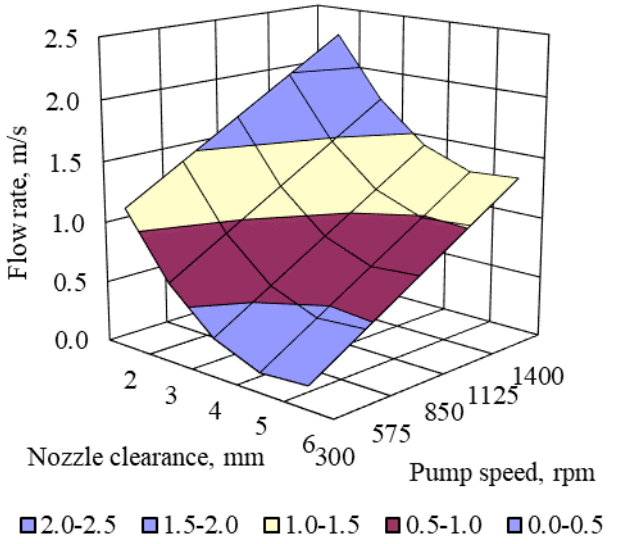

Fig. 7. The dependence of the emulsion flow rate at the exit of the nozzle on the hydro station pump speed and the clearance between the nozzle disks

The analysis of the experimental research of a disk nozzle made it possible to determine the dependence of a speed change in emulsion flow at emulsion flow length on the clearance between the disks of a nozzle.

Fig. 8. The nature of the emulsion flow at a flow rate of 2.08 m/s, the clearance between the nozzle disks of 2 mm and a rotation speed of 1400 min^{-1}

Thus, under the hydro-pump rotation frequency of 1400 min^{-1} the speed of the emulsion flow is described by the equation:

$$\upsilon=3{,}237-0.6805h_0-0.1168l_x+ \\ +0.0604h_0^2+0.0034h_0l_x+0.0019l \quad (13)$$

Under the hydro-pump rotation frequency of 850 min-1 the speed of emulsion flow is described by the equation:

$$\upsilon=2{,}7953-0.6487h_0-0.0977l_x+ \\ +0.0496h_0^2+0.0065h_0l_x+0.0013l_x^2 \quad (14)$$

Under the hydro-pump rotation frequency of 300 min -1 the speed of the emulsion flow is described by the equation:

$$\upsilon=1{,}8887-0{,}5348h_0-0{,}0498l_x+ \\ +0{,}0422h_0^2+0{,}0061h_0l_x+0{,}0003l_x^2 \quad (15)$$

The equations (13, 14, 15) analysis shows that the maximal speed is observed at the exit of an emulsion flow from the nozzle under the clearance of 2 mm between the disks of a nozzle.

For example, when the gap of the nozzle was 2 mm, the immersion depth of the nozzle under the free surface was 47 mm and the rotational speed of the pump of the hydro station was 850 min^{-1} (the pump flow was 0.0014 m^3/s), the flow rate at the beginning was 1.65 m/s (Fig. 9 and 10) and decreased down to 0.14 m/s at a distance of 30 cm from the edge of the nozzle. It fully corresponds to the theoretical studies.

The change in the average flow rate along the length of the flow was obtained as a result of experimental studies corresponding to the change in the average flow rate obtained as a result of theoretical calculations. A slight discrepancy in the results is due to inaccurate measurements in experimental studies.

On the basis of the conducted research, an experimental sample of the circulation reactor with the volume of 0.15 m^3 for biodiesel production (Fig. 11) was made.

The conducted studies can be used while designing of circulating reactors for biodiesel production (table. 5).

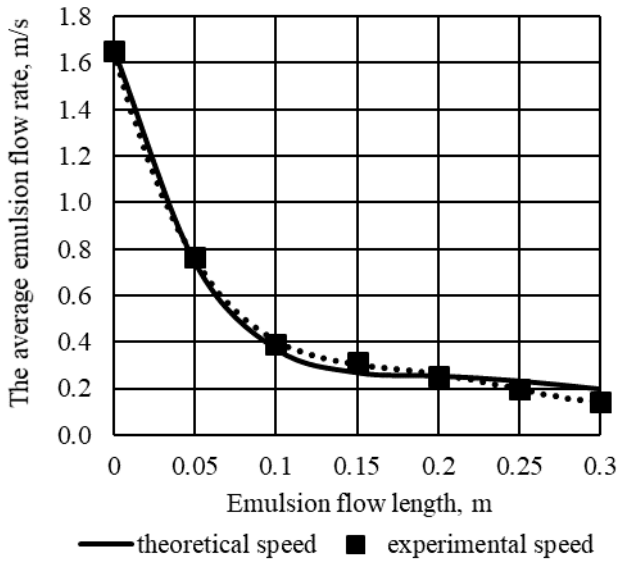

Fig. 9. Change in average flow rate along the flow length

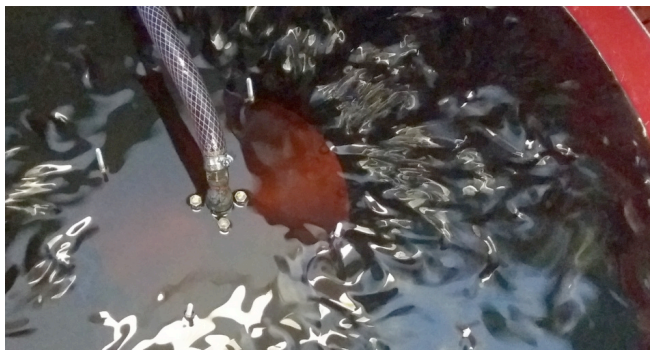

Fig. 10. The nature of the emulsion flow at a flow rate of 1.66 m/sec, the clearance between the nozzle disks of 2 mm and a rotation speed of 850 min^{-1}

Fig. 11. The circulation reactor for biodiesel production

Table 5. Rational parameters of circulation reactors

Parameter	The inner diameter of the reactor D_Z, m					
	0.56	0.8	1.2	1.4	2.2	3
Nominal volume V_P, m3	0.15	0.4	1	2	6.5	18
Effective length of the emulsion flow l_e, m	0.12	0.14	0.17	0.2	0.25	0.3
Diameter of the disk nozzle D_F, m	0.32	0.52	0.86	1	1.7	2.4
The clearance between the nozzle disks h_F, mm	2	2	3	3	4	5
The height of the mixing area H_p m	0.035	0.0402	0.049	0.049	0.071	0.085
The height of the separator H_Z, m	0.65	0.95	1.1	1.6	2	3
Pump flow Q_0, m^3/s	0.0025	0.0047	0.0128	0.0187	0.0517	0.1103
Theoretical pump power N_T, W	300	560	1540	2240	6200	13240
Specific output of the pump n_T, W/m^3	2000	1400	1540	1120	954	736

The disk nozzle can also be used to remove the resulting biodiesel from the circulation reactor after the technological operations of transesterification and settling. The disk nozzle allows to pump the obtained biofuel from the top of the reactor, which makes it impossible to get glycerol into biodiesel. The use of disk nozzles in mixers allows to produce biodiesel by a simplified technology.

4. Conclusion

The disk nozzle is used to form an emulsion flow in which the emulsion components are mixed with the required intensity.

Substantiation of the parameters of the circulating reactor was based on the establishment of the effective length of the emulsion flow. To establish the effective length of the emulsion flow, the axial velocity of the emulsion in the flow sections was determined. Determination of the average speed was carried out by using the principle of conservation of the kinetic energy. For this purpose, the change of the kinetic energy of the annular elements of the emulsion flow at the beginning of the flow (at the outlet of the nozzle) and at the end of the flow (at an effective distance from the nozzle edge) was considered.

As a result of mathematical modeling, it was found that when the hydraulic pump output of 0.0085 m^3/s, the dynamic viscosity of the emulsion of 0.081 Pa s, the emulsion density of 950 kg/m^3, the clearance between the nozzle disks of 2 mm and the depth of immersion of the nozzle, which corresponds to half the height of the mixing area of 0.035 m, the effective emulsion flow length is 0.32 m. It is at a distance of 0.32 m from the nozzle edge that a turbulent mixing mode with the required mixing intensity is observed.

The minimum power consumption of 466 W was observed at a minimum hydroelectric pump speed of 300 min^{-1}, with an increase in the pump speed up to 1400 min^{-1}, the power increases in parabolic dependence and reaches the maximum value of 2460 W.

When changing the speed of the pump, the minimum flow rate at the exit of the nozzle was 0.24 m/s and was observed at a clearance between the nozzle disks of 6 mm and a speed of 300 min^{-1}. The maximum flow rate was 2.08 m/s and was observed at a clearance between the nozzle disks of 2 mm and a rotation frequency of 1400 min^{-1}. Regarding the effect of the clearance between the nozzle disks on the initial flow rate of the emulsion, it can be concluded that the flow rate is reduced by the parabolic dependence with an increase in the clearance between the nozzle disks. When the clearance between the nozzle disks is in excess of 5 mm the initial velocity of the emulsion flow becomes stable and remains practically unchanged with further increase of the clearance between the nozzle disks.

With a clearance between the nozzle disks of 2 mm, the depth of immersion of the nozzle under the free surface of 47 mm and the rotation speed of the hydro station pump of 850 rpm (corresponding to the pump flow of 0.085 m^3/s), the flow rate at the beginning was 1.66 m/s and decreased down to 0.2 m/s at a distance of 30 cm from the nozzle edge. The dynamics of the change in the average flow rate along the length of the flow was obtained as a result of experimental studies consistent with the dynamics of the average flow rate obtained as a result of theoretical calculations.

According to the obtained parameters, an experimental sample of the circulation reactor was made to produce biodiesel with a nominal volume of 0.15 m^3, an internal diameter of 0.56 m, a height of 0.65 m, and a disk nozzle diameter of 0.32 m.

References

[1] A. Harrouz, M. Abbes, I. Colak, and K. Kayisli, Smart grid and renewable energy in Algeria, *2017 IEEE 6th International Conference on Renewable Energy Research and Applications (ICRERA)*, DOI: 10.1109/ICRERA.2017.8191237, San Diego, pp. 1166-1171, 5-8 Novembe 2017, (Conference Paper)

[2] I. Carlucci, G. Mutani, and M. Martino, Assessment of potential energy producible from agricultural biomass in the municipalities of the Novara plain, 2015 International Conference on Renewable Energy Research and Applications (ICRERA), DOI: 10.1109/ICRERA.2015.7418636, Palermo, pp. 1394-139822- 25, Novembe, (Conference Paper)

[3] S. Dewang, Suriani, S. Hadriani, Diana, E.S. Lestari, and Bannu, Viscosity and calorie measurements of biodiesel production from Callophyllum Inophyllum L using catalyst and time variations for stirring in tansesterfication process, 2017 IEEE 6th International Conference on Renewable Energy Research and Applications (ICRERA), DOI: 10.1109/ICRERA.2017.8191157, San Diego, pp. 734-738, 5-8 Novembe 2017, (Conference Paper)

[4] G.A. Golub, S.M. Kukharets, Y.D Yarosh, and V.V. Kukharets. Integrated use of bioenergy conversion technologies in agroecosystems, INMATEH – Agricultural Engineering, vol. 51, no. 1, pp. 93–100, January 2016. (Article)

[5] M. Mofijur, M.G. Rasul, J. Hyde, A.K. Azad, R. Mamat, and M.M.K. Bhuiya, Role of biofuel and their binary (diesel–biodiesel) and ternary (ethanol–biodiesel–diesel) blends on internal combustion engines emission reduction, Renewable and Sustainable Energy Reviews, DOI: doi.org/10.1016/j.rser.2015.08.046, vol. 53, pp. 265-278, January 2016. (Article)

[6] R. Arslan, and Yahya Ulusoy, Utilization of waste cooking oil as an alternative fuel for Turkey, 2016 IEEE International Conference on Renewable Energy Research and Applications (ICRERA), DOI: 10.1109/ICRERA.2016.7884526, Birmingham, pp. 149-152, 20-23 Novembe 2016, (Conference Paper)

[7] R. Sakthivel, K. Ramesh, R. Purnachandran, and P. Mohamed Shameer, A review on the properties, performance and emission aspects of the third generation biodiesels, Renewable and Sustainable Energy Reviews, DOI: 10.1016/j.rser.2017.10.037, vol. 52, part 3, pp. 2970-2992, February 2017. (Article)

[8] J. E, M. Pham, D. Zhao, Y. Deng, D. Le, W. Zuo, H. Zhu, T. Liu, Q. Peng, and Z. Zhang, Effect of different technologies on combustion and emissions of the diesel engine fueled with biodiesel: A review, Renewable and Sustainable Energy Reviews, DOI: 10.1016/j.rser.2017.05.250, vol. 80, pp. 620-647, December 2017. (Article)

[9] Y. Cheng, S. Li, J. Liggio, K. Hayden, Y. Han, C. Stroud, T. Chan, and M. Poitras, The effects of biodiesels on semivolatile and nonvolatile particulate matter emissions from a light-duty diesel engine, Environmental Pollution, DOI: 10.1016/j.envpol.2017.06.014, vol. 230, pp. 72-80, November 2017. (Article)

[10] G. Golub, S. Kuharets, O. Osyipchuk, V. Kuharets, Analysis of the process of biodiesel production and substantiation of the main parameters of the reactor-separator. Motrol, Commission of motorization and energetics in agriculture, vol. 17(9), pp. 149–155, 2016. (Article)

[11] Md Ehsan, Md Tofajjal Hossain Chowdhury, Production of Biodiesel Using Alkaline Based Catalysts From Waste Cooking Oil: A Case Study, Procedia Engineering, DOI: 10.1016/j.proeng.2015.05.042, vol. 105, pp. 638-645, 2015. (Article)

[12] T. Takata, O. Nakagoe, and S. Tanabe, Effect of Al loading on CaO catalysts for biodiesel production. 2012 International Conference on Renewable Energy Research and Applications (ICRERA), DOI:10.1109/icrera.2012.647735520-23 11-14, Nagasaci, Novembe 2012, (Conference Paper)

[13] G. Baskar, R. Aiswarya, Trends in catalytic production of biodiesel from various feedstocks, Renewable and Sustainable Energy Reviews, DOI: 10.1016/j.rser.2015.12.101, vol. 57, pp. 496-504, May 2016. (Article)

[14] Z. Qiu, L. Zhao, L. Weatherley, Process intensification technologies in continuous biodiesel production, Chemical Engineering and Processing: Process Intensification, DOI: 10.1016/j.cep.2010.03.00549, vol. 49, is. 4, pp. 323-330, April 2010. (Article)

[15] A. Amelio, T. Van de Voorde, C. Creemers, J. Degrève, S. Darvishmanesh, P. Luis, and B. Van der Bruggen, Comparison between exergy and energy analysis for biodiesel production, Energy, DOI: 10.1016/j.energy.2016.01.018, vol. 98, pp. 135-145, March 2016. (Article)

[16] B. Rahmat, I. Setiasih, R. Kastaman, Biodiesel Reactor Design with Glycerol Separation to Increase Biodiesel Production Yield. Makara Journal of Technology, DOI: 10.7454/mst.v17i1.255, vol. 17(1), pp. 11-16, February 2013. (Article)

[17] K. Somnuk, T. Prasit, G. Prateepchaikul, Effects of mixing technologies on continuous methyl ester production: Comparison of using plug flow, static mixer, and ultrasound clamp, Energy Conversion and Management, DOI: 10.1016/j.enconman.2017.02.066, vol. 140, pp. 91-97, May 2017. (Article)

[18] S. Drahniev, Fuzzy modeling of the technological process of biodiesel production, Scientific Bulletin of National Agricultural University (Kyiv/Ukraine), vol.117, pp. 350-357, 2007. (Article)

[19] S. Drahniev, Experimental researches of technological parameters of the esterification process of vegetable oils, Scientific Bulletin of National University of Life and Environmental Sciences of Ukraine (Kyiv/Ukraine), vol.144, no.3, pp. 163–172, 2010. (Article)

[20] S. Drahniev, S. Kukharets, Verification of structural parameters of periodic reactor for esterification of vegetable oils, Scientific Bulletin of National University of Life and Environmental Sciences of Ukraine (Kyiv/Ukraine), vol.144, no.4, pp. 334-342, 2010. (Article)

[21] J. K. Poppe, R. Fernandez-Lafuente, R. C. Rodrigues, and M. Antônio Záchia Ayub, Enzymatic reactors for biodiesel synthesis: Present status and future prospects, Biotechnology Advances, DOI: 10.1016/j.biotechadv.2015.01.011, vol. 33(5), pp. 511–525, September–October 2015. (Article)

[22] J. Xu, C. Liu, M. Wang, L. Shao, L. Deng, K. Nie, and F. Wang, Rotating packed bed reactor for enzymatic synthesis of biodiesel, Bioresource Technology, DOI: 10.1016/j.biortech.2016.10.045, vol. 224, pp. 292–297, January 2017. (Article)

[23] R. Alamsyah, H. Loebis, Design and Technical Testing for Crude Biodiesel Reactor Using Dry Methods: Comparison of Energy Analysis. Energy Procedia, DOI: 10.1016/j.egypro.2014.01.219 vol. 47, pp. 235-241, 2014. (Article)

[24] I. Atadashi, Purification of crude biodiesel using dry washing and membrane technologies, Alexandria Engineering Journal, DOI: 10.1016/j.aej.2015.08.005, vol. 54, is. 4, pp. 1265–1272, December 2015. (Article)

[25] M. Noriega, P. Narváez, J. Cadavid, and A. Habert, Modeling of biodiesel production in Liquid-Liquid Film Reactors including mass transfer effects, Fuel Processing Technology, DOI: 10.1016/j.fuproc.2017.08.008, vol. 167, pp. 524-534, December 2017. (Article)

[26] B. Likozar, A. Pohar, and J. Levec, Transesterification of oil to biodiesel in a continuous tubular reactor with static mixers: Modelling reaction kinetics, mass transfer, scale-up and optimization considering fatty acid composition, Fuel Processing Technology, DOI: 10.1016/j.fuproc.2015.10.035, vol. 142, pp. 326-336, February 2016. (Article)

[27] Crudo, D., Bosco, V., Cavaglià, G., Grillo, G., Mantegna S., and Cravotto, G., Biodiesel production process intensification using a rotor-stator type generator of hydrodynamic cavitation, Ultrasonics Sonochemistry, DOI: 10.1016/j.ultsonch.2016.05.001, vol. 33, pp. 220-225, November 2016. (Article)

[28] A. Hajinezhad, and S. Sina Hosseini, Ultrasound Assisted Biodiesel Production from Eruca Sativa as an Indigenous Species in Iran, Internatıonal Journal of Renewable Energy Research, Vol.7, No.2, January 2017. (Article)

[29] R. Alenezi, R. C. D. Santos, S. Raymahasay, and G. A. Leeke, Improved biodiesel manufacture at low temperature and short reaction time, Renewable Energy, DOI: 10.1016/j.renene.2012.11.019, vol. 53, pp. 242-248, may 2013. (Article)

[30] P. Sungwornpatansakul, J. Hiroi, Y. Nigahara, T. Kaushalya Jayasinghe, K. Yoshikawa, Enhancement of biodiesel production reaction employing the static mixing, Fuel Processing Technology, DOI: 10.1016/j.fuproc.2013.04.019, vol. 116, pp. 1-8, December 2013. (Article)

[31] G. Golub, S. Kukharets, V. Chuba, M. Pavlenko, and Y. Yarosh, Rationale for the parameters of equipment for production and use of biodiesel in agricultural production. Eastern-European Journal of Enterprise Technologies, DOI: 10.15587/1729-4061.2017.95937, no. 2/1 (86), pp. 28-33, March 2017. (Article)

[32] Z. Sterbacek, P. Tausk, Mixing in the chemical industry, Published by Pergamon Press Ltd, Oxford, 1965. (Book)

[33] P. Kundu, I. Cohen, D. Dowling, Fluid Mechanics, Academic Press, Boston/USA, June 2016. (Book)

View publication stats